Properties and Structure of Binary PbO-GaO$_{1.5}$ Glasses as the Base of Nonlinear Optical Multicomponent Glasses

Fumiaki Miyaji*, Kiyoharu Tadanaga* and Sumio Sakka*

The densities, refractive indices, glass-transition temperature, T$_g$, IR and Raman spectra, third-order nonlinear susceptibility, $\chi^{(3)}$, and crystallization behavior have been investigated for non-conventional PbO-GaO$_{1.5}$ glasses, which are regarded as bases of nonlinear optical glasses, and their structure has been discussed. Some of the properties were compared with those of the corresponding silicate glass. The density and refractive index increased and the T$_g$ decreased with increasing PbO content of the glasses. The cutoff wavelength in IR region of 67PbO·33GaO$_{1.5}$ glass was longer than that of 67PbO·33SiO$_2$ glass. The $\chi^{(3)}$ value of 67PbO·33GaO$_{1.5}$ glass was about 1.7 times higher than that of 67PbO·33SiO$_2$ glass. Heating of the glasses caused the precipitation of lead oxides; α-PbO crystal and β-PbO-like solid solution were formed at the first stage of crystallization of 50PbO·50GaO$_{1.5}$ and 60PbO·40GaO$_{1.5}$ glasses, respectively. Structural consideration based on the Raman spectra indicated that Ga^{3+} ions are tetrahedrally coordinated and the Ga-O bond strength decreases with increasing PbO content. It was also indicated that the sites next nearest to Ga^{3+} ions are occupied by not only Pb^{2+} ions but also Ga^{3+} ions in even very high-PbO compositions and the fraction of non-bridging oxygens in GaO$_4$ tetrahedra decreases with increasing PbO content.

KEY WORDS: PbO-GaO$_{1.5}$ glasses/ Non-conventional glasses/ Properties/ Structure/ Nonlinear optical glasses

1. INTRODUCTION

Recently, non-conventional oxide glasses are attracting much attention from practical application to optical devices as well as the science of glass formation and structure. Non-conventional oxide glasses are defined as glasses which do not contain so-called glass-forming oxide, such as SiO$_2$, B$_2$O$_3$, P$_2$O$_5$, GeO$_2$ or As$_2$O$_3$, but consist of combinations of so-called intermediate and network-modifying oxides, such as Al$_2$O$_3$, Ga$_2$O$_3$, TiO$_2$, Nb$_2$O$_5$, Ta$_2$O$_5$, TeO$_2$, PbO and Bi$_2$O$_3$.[1-11] Some of such glasses are expected as new functional glasses for their pronounced optical[1-5,8] and electrical[9,11] properties. Specifically, PbO-GaO$_{1.5}$ binary glasses are regarded as the base of nonlinear optical glasses.

Since Dumbaugh exploited non-conventional PbO-Bi$_2$O$_3$-Ga$_2$O$_3$ glasses for high refractive index and IR-transmitting materials,[8] there have been many structural studies and optical measurements for ternary and multicomponent glasses based on PbO-GaO$_{1.5}$ binary glasses. The determination of the glass-forming region, density, refractive index, cutoff wavelength in IR and UV-VIS region and third order nonlinear susceptibility $\chi^{(3)}$ of the MO$_x$-PbO-GaO$_{1.5}$ (M = Ti,Nb,W) ternary systems,[12] and structural studies of PbO-BiO$_{1.5}$-

---

* 宮路史明, 忠永清治, 作花済夫 : Laboratory of Ceramic Chemistry, Institute for Chemical Research, Kyoto University, Uji, Kyoto-fu 611, Japan

$GaO_{1.5}$ glasses by IR, Raman[13] and ^{71}Ga NMR[14] spectroscopies have been reported.

The $PbO-GaO_{1.5}$ binary system has a wide glass-forming region in spite of both oxide components being intermediate oxides.[15] In the present study, the density, refractive index, glass-transition temperature, T_g, IR transmission, third-order nonlinear susceptibility, $\chi^{(3)}$, and crystallization behavior have been investigated for $PbO-GaO_{1.5}$ glasses, which are regarded as bases of nonlinear optical glasses, and their structure has been discussed on the basis of Raman spectra.

2. EXPERIMENTAL

2.1 Sample preparation

A 10 g glass batch consisting of analytical grade reagents of PbO and Ga_2O_3 was put into a platinum crucible, covered with a lid and melted at 1000–1400°C for 15 min in an electric furnace. The melt was poured on a brass plate and quickly pressed to a sheet by another brass plate. Light yellow-orange-colored transparent glasses with 1–2 mm thick were prepared for the composition $xPbO\cdot(100-x)GaO_{1.5}$ (x = 40,50,60,67,70). In this paper, the glass composition is represented by mol% of the components, PbO and $GaO_{1.5}$.

2.2 Density, refractive index and IR transmission

The density of the glasses was measured by the pycnometric method using water as immersion liquid.

The refractive index was measured in the range from 470 to 1100 nm by a Mizojiri-Kogaku model DVA-36VW ellipsometer.

The cutoff wavelength in IR region was determined by a Nippon-Bunko model FT/IR-5M infrared spectrometer. The cutoff wavelength was determined as the wavelength where the transmittance of a 1mm thick sample was 50%.

2.3 Nonlinear optical properties

The third-order nonlinear susceptibility, $\chi^{(3)}$, was determined by THG (Third Harmonic Generation) method using the apparatus assembled by Tokyo Instruments Co. The measurements were made with a Q-switched Nd:YAG laser operated at 1.064 μm of fundamental wavelength. The light of 1.907 μm wavelength was obtained by the Raman shift in a high-pressure hydrogen cell. The pulse duration was 10 ns. The intensity of THG at 0.635 μm was estimated by measuring Maker fringe patterns.[16]

2.4 Crystallization

The glass-transition temperature, T_g, and the crystallization onset temperature, T_x, of the glasses were measured by a Rigaku-Denki model Thermoflex TG 8110 DSC apparatus. The measurements were made on powder samples of about 40 mg under air atmosphere with heating rate of 10°C/min.

The sheets of $50PbO\cdot50GaO_{1.5}$ and $60PbO\cdot40GaO_{1.5}$ glasses were put on platinum plates and heated at various temperatures for 20 h. The precipitated phases were identified by X-ray diffraction using a Rigaku-Denki model Geiger flex RAD II-A diffractometer.

2.5 Measurements and analysis of Raman spectra

Raman spectra of the glasses were measured with a Nippon Bunko model JASCO NR-1000S laser Raman spectrometer using the 514.5 nm line of an Ar^+ laser as the exciting beam. The power was adjusted to 250–550 mW. The resolution and the precision of

wavenumber are within 1 cm^{-1}. The measured Raman spectra were corrected for the intensity of Reyleigh and Raman scatterings and normalized according to the method described by Long.[17] Deconvolution was made on the curves for 50–850 cm^{1-} by the least-squares fitting based on the assumption that each Raman band takes a curve of Gaussian distribution.

3. RESULTS

3.1 Density, refractive index and IR transmission

Fig. 1 shows the density of PbO-GaO$_{1.5}$ glasses. The closed semicircles at 0 and 100 mol% PbO represent the densities of amorphous GaO$_{1.5}$ (a-GaO$_{1.5}$) and amorphous PbO (a-PbO) estimated by extrapolation of the densities of Cs$_2$O-Ga$_2$O$_3$[18] and PbO-B$_2$O$_3$[19] glasses, respectively. The densities of amorphous GaO$_{1.5}$ and amorphous PbO estimated by extrapolation of present data for PbO-GaO$_{1.5}$ glasses are 4.52 and 8.43 gcm^{-3}, respectively, agreeing well with the values mentioned above.

The refractive indices of PbO-GaO$_{1.5}$ glasses at 638 nm are shown in Fig. 2. The refractive index linearly increases from about 2.1 for the composition 40PbO·60GaO$_{1.5}$ to
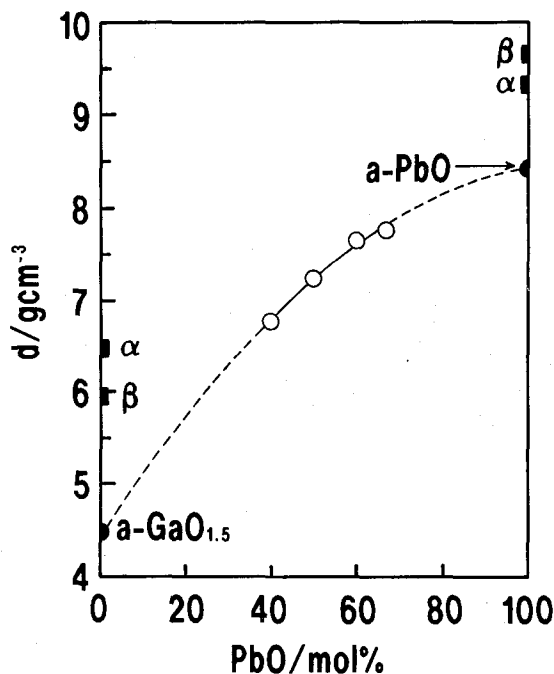

Fig. 1 Density of PbO-GaO$_{1.5}$ glasses. a-GaO$_{1.5}$ and a-PbO denote amorphous GaO$_{1.5}$ and amorphous PbO, respectively. The broken line shows extrapolations of the line obtained by the least squares fitting with second-order function. Closed rectangles denote the densities of crystals.
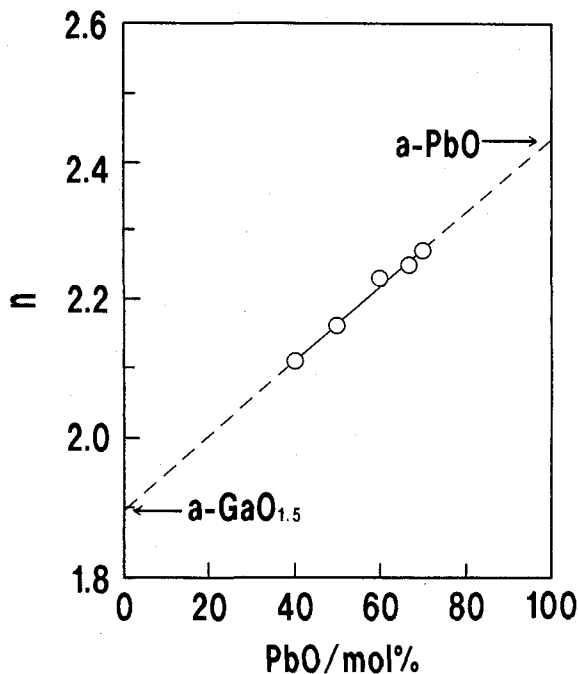
Fig. 2 Refractive indices of PbO-GaO$_{1.5}$ glasses. The measurements were made at 638 nm with a He-Ne laser. a-GaO$_{1.5}$ and a-PbO denote amorphous GaO$_{1.5}$ and amorphous PbO, respectively. The broken line shows extrapolations of the line obtained by least squares fitting with first-order function.

about 2.3 for the composition 70PbO·30GaO$_{1.5}$ with increasing PbO content. The broken line in the figure is the linear least-squares fitting. The refractive indices of amorphous GaO$_{1.5}$ and amorphous PbO estimated by extrapolation are 1.90 and 2.43, respectively.

The molar refraction, R$_M$, of PbO-GaO$_{1.5}$ glasses has been calculated from equation (1)

$$R_M = \frac{M}{d} \frac{n^2 - 1}{n^2 + 2} \tag{1}$$

where M, d and n represent the molecular weight per unit composition, the density and the refractive index, respectively. Fig. 3 shows the molar refraction of PbO-GaO$_{1.5}$ and PbO-SiO$_2$ glasses. The closed circles and the solid line denote the experimental values and the calculated curve for PbO-GaO$_{1.5}$ glasses, respectively. The open circles denote the R$_M$ calculated from the data of densities and refractive indices of PbO-SiO$_2$ glasses.[20] The broken line is drawn by least-squares fitting to the data of R$_M$ (open circles) with the second-order function. It is found that the R$_M$ of amorphous PbO is 16.4 and 16.5 for the PbO-GaO$_{1.5}$ and PbO-SiO$_2$ glasses, respectively.

Fig. 4 shows the dependence of refractive indices of 67PbO·33GaO$_{1.5}$ and 67PbO·33SiO$_2$ glasses on wavelength. It is seen that 67PbO·33GaO$_{1.5}$ glass shows a higher
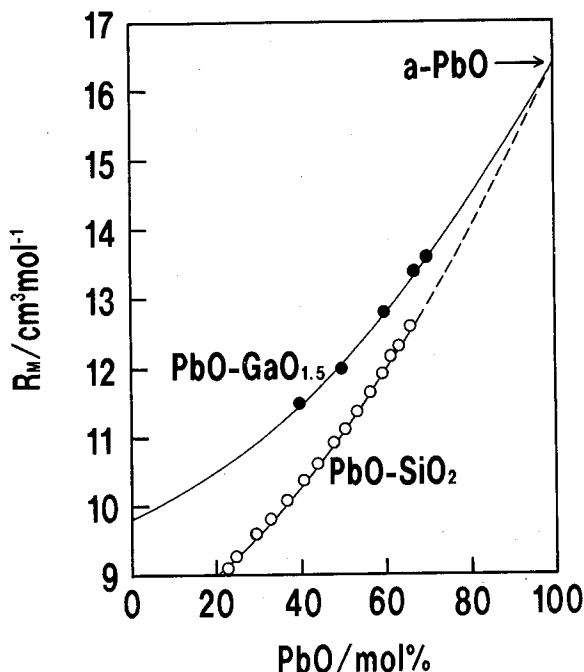
Fig. 3 Molar refraction of PbO-GaO$_{1.5}$ and PbO-SiO$_2$ glasses. The curves have been obtained by least-squares fitting with second-order function. The data for PbO-SiO$_2$ glasses denoted by open circles are from reference (20).

refractive index and larger dispersion than those of 67PbO·33SiO$_2$ glass in the wavelength range of the present measurements.

Fig. 5 shows the IR absorption spectra of (a) 67PbO·33GaO$_{1.5}$ and (b) 67PbO·33SiO$_2$ glasses. The 67PbO·33GaO$_{1.5}$ glass shows a transmittance higher than 50% up to about 7.1 μm, whereas the 67PbO·33SiO$_2$ glass does only up to 4.5 μm.

3.2 Nonlinear optical properties

The nonlinear susceptibility, $\chi^{(3)}$, was obtained by referring to the measurement for SiO$_2$ glass with 1 mm thick. The following equation was used.[21]

$$\chi^{(3)}(\text{sample}) = \chi^{(3)}(\text{SiO}_2) \frac{l_c(\text{SiO}_2)}{l_c(\text{sample})} \left(\frac{I(\text{sample})}{I(\text{SiO}_2)} \right)^{1/2} \tag{2}$$

where l_c and I represent the coherent length and the THG intensity, respectivey. l_c is calculated from

$$l_c = \lambda_p/[6(n_{3\omega} = n_\omega)] \tag{3}$$

where λ_p represents the wavelength of pumping light and $n_{3\omega}$ and n_ω the refractive indices at 0.635 and 1.907 μm, respectively. $l_c(\text{SiO}_2)$ and $\chi^{(3)}(\text{SiO}_2)$ were assumed to be 18.4 μm and 2.8×10^{-14} esu, respectively, in the calculation.[22] n_ω was obtained from the extrapolation of linear plots of $1/(n^2 - 1)$ vs. $1/\lambda^2$.
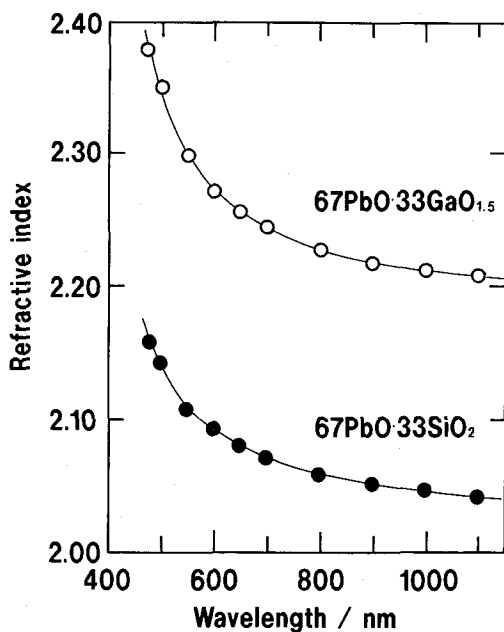
Fig. 4 The dependence of refractive indices of $67PbO \cdot 33GaO_{1.5}$ and $67PbO \cdot 33SiO_2$ glasses on wavelength. The measurements were made with a halogen lamp combined with monochromator.
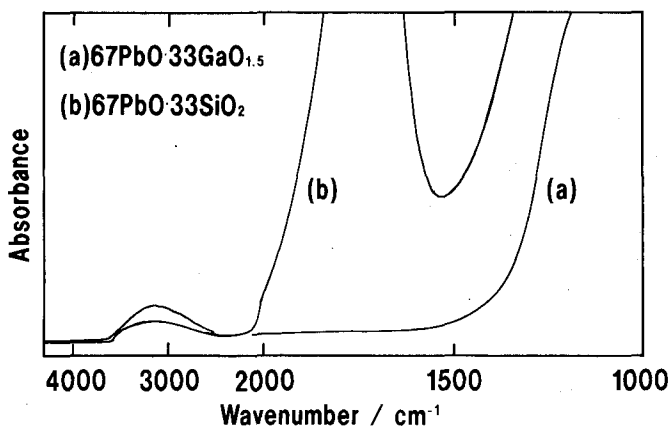

Fig. 5 IR absorption spectra of (a) $67PbO \cdot 33GaO_{1.5}$ and (b) $67PbO \cdot 33SiO_2$ glasses. The thickness of samples was 1 mm.

$\chi^{(3)}$ can be calculated empirically,[23]

$$n_2(10^{-13} \text{ esu}) = \frac{68(n_d - 1)(n_d^2 + 2)^2}{\nu[1.52 + (n_d^2 + 2)(n_d + 1)\nu/6n_d]^{1/2}} \qquad (4)$$

$$\chi^{(3)}(10^{-13} \text{ esu}) = \frac{n \times n_2}{12\pi} \qquad (5)$$

where n_2, n_d and ν represent the nonlinear refractive index, the refractive index at 587.6 nm and the Abbe number. Eq.(4) indicates that n_2 increases with increasing n_d and reciprocal ν.

The Maker fringe patterns of (a) 67PbO·33GaO$_{1.5}$ and (b) 67PbO·33SiO$_2$ glasses are shown in Fig. 6. Both glasses show about 20 times higher THG intensities than that of SiO$_2$ glass. It is found that the oscillation period, reflecting the coherent length, of 67PbO·33GaO$_{1.5}$ glass is shorter than that of 67PbO·33SiO$_2$ glass.

The experimental and calculated $\chi^{(3)}$ values are listed in Table 1. The experimental $\chi^{(3)}$ value of 67PbO·33GaO$_{1.5}$ glass is about 30 times higher than that of SiO$_2$ glass and about 1.7 times higher than those of 67PbO·33SiO$_2$ and 60PbO·40BO$_{1.5}$ glasses. All the
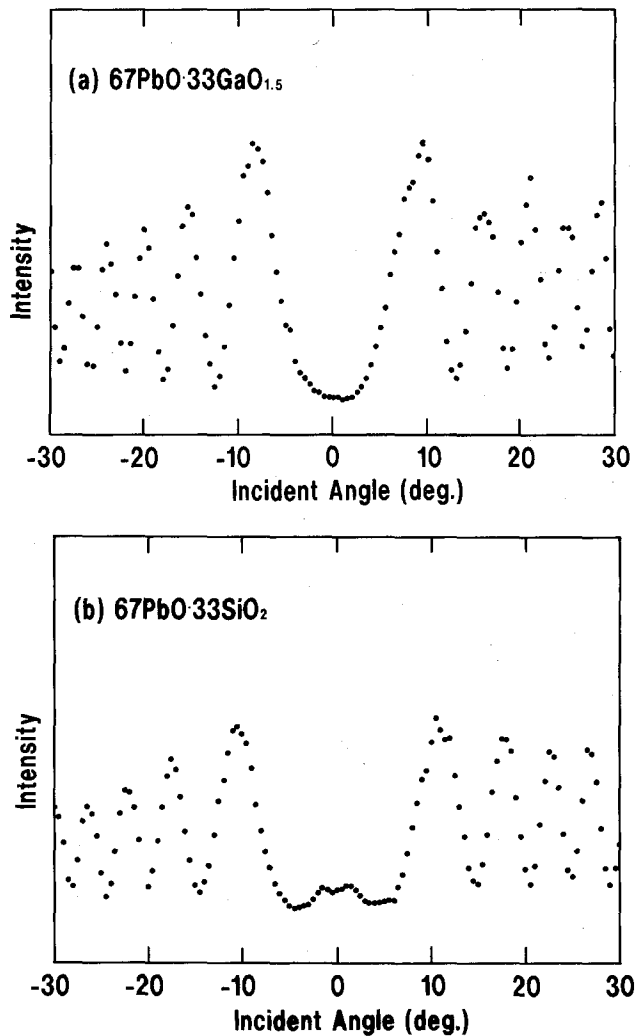

Fig. 6 Maker fringe patterns of (a) 67PbO·33GaO$_{1.5}$ and (b) 67PbO·33SiO$_2$ glasses.

Table 1　Nonlinear optical properties of PbO-MO$_x$ glasses

Glass	$n_{3\omega}$	n_ω	I/I(SiO$_2$)	l_c	$\chi^{(3)}/10^{-13}$ esu	
					Obs.	Cal.
67PbO·33GaO$_{1.5}$	2.260	2.159	22	3.14	7.7	4.5
67PbO·33SiO$_2$	2.087	2.022	19	4.86	4.6	1.8
60PbO·40BO$_{1.5}$	2.107	2.034	16	4.36	4.7	2.2
SiO$_2$*				18.4	0.28	

*cited from reference (22)

calculated $\chi^{(3)}$ values are much lower than corresponding experimental $\chi^{(3)}$ values.

3.3　Crystallization

Fig. 7 shows the DSC curves of PbO-GaO$_{1.5}$ glasses. One sharp exothermic peak is observed at 526.2 and 512.8°C in the curves of 40PbO·60GaO$_{1.5}$ and 50PbO·50GaO$_{1.5}$ glasses, respectively. A broad peak and a relatively sharp peak are observed at 479.3 and 524.0°C, respectively, for 60PbO·40GaO$_{1.5}$ glass. A broad peak and two small peaks are
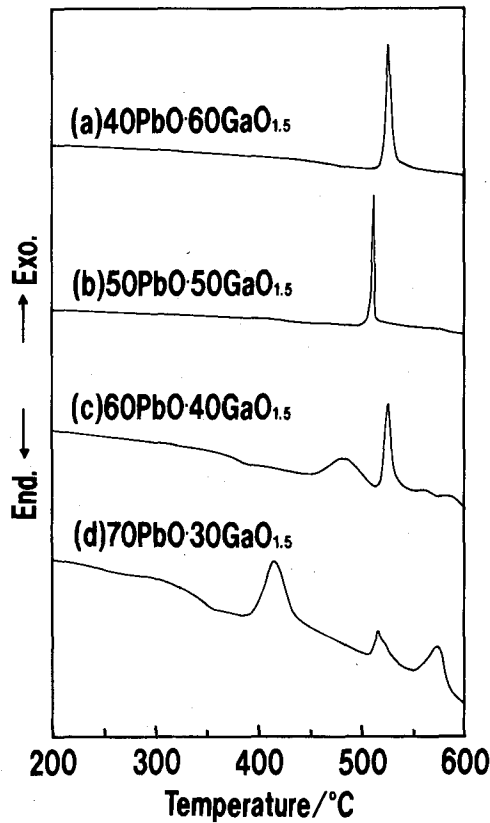

Fig. 7　DSC curves of (a) 40PbO·60GaO$_{1.5}$, (b) 50PbO·50GaO$_{1.5}$, (c) 60PbO·40GaO$_{1.5}$ and (d) 70PbO·30GaO$_{1.5}$ glasses. The heating rate was 10°C/min.
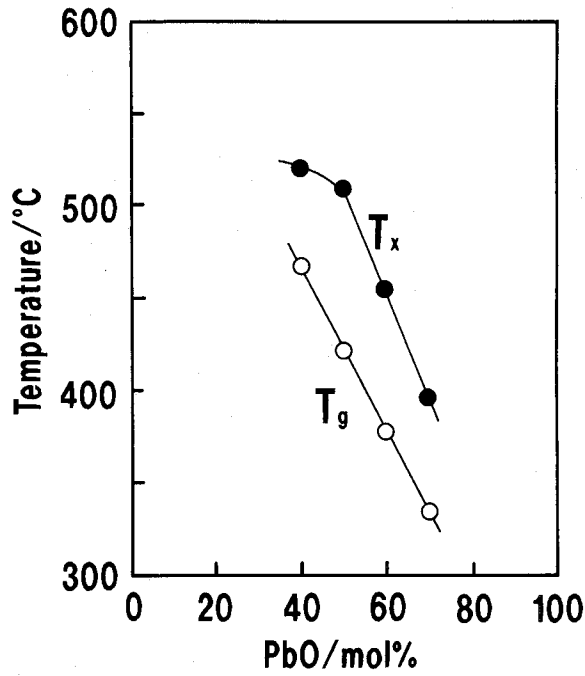
Fig. 8 Glass-transition temperature, T$_g$, and crystallization onset temperature, T$_x$, of PbO-GaO$_{1.5}$ glasses. The heating rate was 10°C/min.
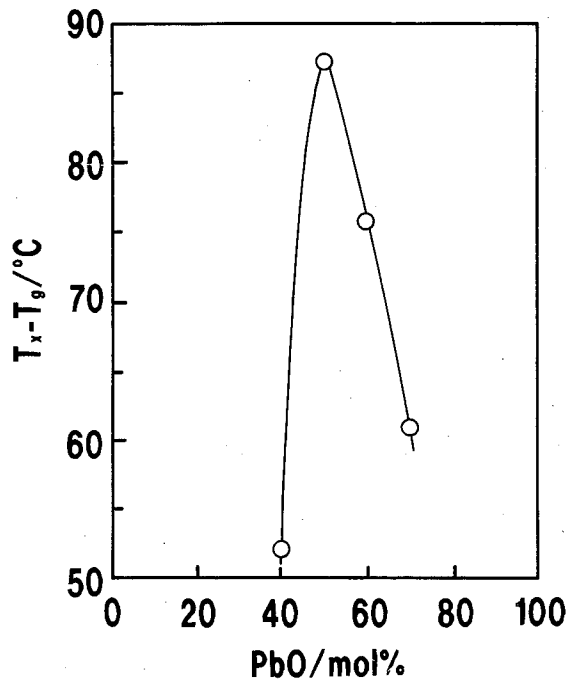

Fig. 9 The dependence of (T$_x$-T$_g$) of PbO-GaO$_{1.5}$ glasses on the PbO content.

observed at 414.1, 515.9 and 572.2°C, respectively, for 70PbO·30GaO$_{1.5}$ glass. Fig. 8 shows the glass-transition temperature, T_g, and the crystallization onset temperature, T_x, of PbO-GaO$_{1.5}$ glasses. The T_g linearly decreases with increasing PbO content. The T_x of 50PbO·50GaO$_{1.5}$ glass is only slightly smaller than that of 40PbO·60GaO$_{1.5}$ glass, and linearly and drastically decreases for the compositions containing more than 50 mol% PbO. Fig. 9 shows the dependence of (T_x-T_g) of PbO-GaO$_{1.5}$ glasses on the PbO content. The (T_x-T_g), which is regarded as a measure of ease of glass formation, shows the maximum value of about 87°C at the composition of 50 mol% PbO.

Figs. 10 and 11 show the X-ray diffraction patterns of 50PbO·50GaO$_{1.5}$ and 60PbO·40GaO$_{1.5}$ glasses heated at various temperatures for 20 h, respectively. The figures suggest that the process of crystallization is appreciably different in these two compositions.

For the 50PbO·50GaO$_{1.5}$ composition, the major part of sample remains amorphous at 450°C. α-PbO crystal, the low-temperature form of PbO crystal, is precipitated at 500°C. β-PbO, high-temperature form of PbO crystal, and PbGa$_2$O$_4$ crystals are formed at 600°C and the peaks of α-PbO become small. The strongest peaks of β-PbO and PbGa$_2$O$_4$ crystals have almost the same d-spacings, being overlapped at about $2\theta = 28.5°$. Almost no change is observed for the diffraction patterns at higher temperatures than 600°C.

For the 60PbO·40GaO$_{1.5}$ composition, only β-PbO crystal is precipitated at 430°C. The peak intensity of β-PbO increases and a small amount of α-PbO begins to precipitate at 500°C. The peaks of β-PbO become small and those of α-PbO become strong at 550°C. PbGa$_2$O$_4$ crystal is formed at 600°C. It is seen that the peaks of β-PbO become small and those of α-PbO become strong at higher temperatures than 700°C.
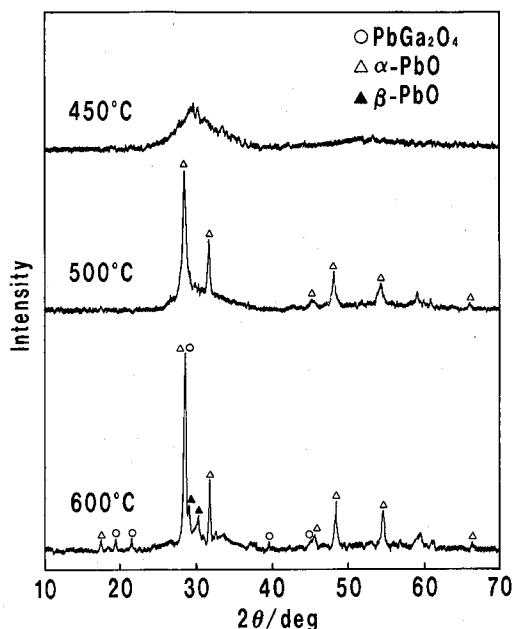

Fig. 10 X-ray diffraction patterns of 50PbO·50GaO$_{1.5}$ glass heated at various temperatures for 20 h.
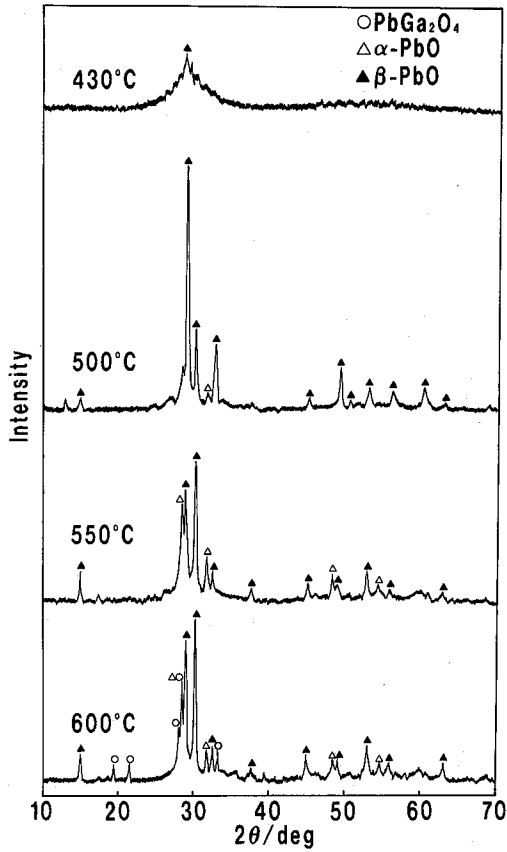
Fig. 11   X-ray diffraction patterns of 60PbO·40GaO$_{1.5}$ glass heated
          at various temperatures for 20 h.

3.4   Raman spectra

All the Raman spectra of PbO-GaO$_{1.5}$ glasses showed similar profiles and continuously varied with the composition.   The Raman spectrum of each glass was deconvoluted to six bands.   Fig. 12 shows the profile of deconvoluted peaks for 40PbO·60GaO$_{1.5}$ glass.   The data of Gaussian deconvolution of Raman spectra are shown in Table 2.   The devonvoluted six bands are denoted as 130 cm^{-1}-, 200 cm^{-1}-, 400 cm^{-1}-, 510 cm^{-1}-, 620 cm^{-1}- and 700 cm^{-1}-band.

Table 2   Numerical results of Gaussian fitting of Raman spectra

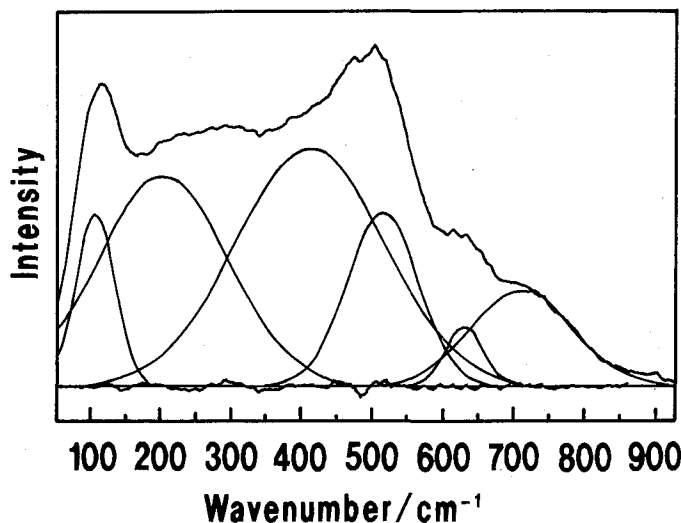| Composition	Peak wavenumbers of each deconvoluted band/cm^{-1}						Intensity ratio	
	130	200	400	510	620	700	I(400)/ I(510)	I(620,700)/ I(510)
40PbO·60GaO$_{1.5}$	106	203	413	515	630	711	2.8	0.96
60PbO·40GaO$_{1.5}$	130	185	392	510	620	696	3.3	0.63
67PbO·33GaO$_{1.5}$	132	184	377	506	620	705	2.8	0.53

Fig. 12   Peak deconvolution of Raman spectra of $40PbO \cdot 60GaO_{1.5}$ glass. The oscillation around the base line shows the residual in least-squares calculation.

4. DISCUSSION

4.1 Density

The densities of amorphous $GaO_{1.5}$ and amorphous PbO estimated by extrapolation shown in Fig. 1 are considerably lower than the densities of various $GaO_{1.5}$ and PbO crystals denoted as closed rectangles, that is, 6.48, 5.95, 9.33 and $9.64\,gcm^{-3}$ for α-Ga_2O_3, β-Ga_2O_3, α-PbO and β-PbO, respectively.

α-Ga_2O_3 has the oxygen ions in approximately hexagonal close-packed array with all the Ga^{3+} ions octahedrally coordinated to O^{2-} ions.[24]   On the other hand, β-Ga_2O_3 consists of GaO_6 octahedra and GaO_4 tetrahedra, which results in lower density of β-Ga_2O_3 than that of α-Ga_2O_3.[24]   More than 24% lower density of extrapolated amorphous $GaO_{1.5}$ compared with crystalline Ga_2O_3 is attributed to the lower coordination number of Ga^{3+} ions in the amorphous state.   These indicate that almost all the Ga^{3+} ions may be present in GaO_4 tetrahedra.

α-PbO and β-PbO consist of PbO_4 square pyramids.[25]   The density of amorphous PbO estimated by extrapolation is about only 10% smaller than crystalline PbO.   This small difference is explained by assuming that the oxygen coordination number of Pb^{2+} ions in amorphous PbO is close to that in crystalline PbO, that is, three or four.[13]   The densities of PbO-$GaO_{1.5}$ glasses measured in the present work agree with those reported by Lapp et al.[26]

4.2 Refractive index

The refractive index of PbO-$GaO_{1.5}$ glasses linearly increases with increasing PbO content.   It has been reported that the refractive index of Ga_2O_3 glass spheres prepared by laser spin melting is 1.91.[27]   This value agrees with the present value of 1.90 for amorphous $GaO_{1.5}$ estimated by extrapolation.   It can be expected that the refractive index of amor-

phous Ga$_2$O$_3$ is not so high as to achieve high-refractive index glassby itself. However, Ga$_2$O$_3$ constituent is expected to make a large contribution to the refractive index compared with conventional network-forming oxides such as SiO$_2$, B$_2$O$_3$ and P$_2$O$_5$. The higher refractive index and dispersion of 67PbO·33GaO$_{1.5}$ glass than those of 67PbO·33SiO$_3$ glass is attributed to the behavior of Ga$_2$O$_3$. On the other hand, the refractive index of amorphous PbO estimated by extrapolation is lower than those of crystalline PbO by about 0.1 – 0.2. This indicates that the packing of oxygens around Pb^{2+} ions in glasses is not dense compared with that in crystals. It can be said, however, that a series of PbO-GaO$_{1.5}$ glass is one of the highest refractive index oxide glasses at present.

The molar refraction of amorphous PbO calculated from the PbO-GaO$_{1.5}$ glasses is consistent with that from the PbO-SiO$_2$ glasses. This may result from the fact that Pb^{2+} ions have a similar coordination number, that is, three or four for both kinds of glasses in the high-PbO composition.[13] The rate of increase in R$_M$ of glass with the PbO content increases with increasing PbO content for both kinds of glasses, which seems to be in conflict with the increase of Pb^{2+} ions having smaller coordination number in the high-PbO region. However, this can be explained by assuming that the refractive indices of PbO-based glasses may be largely determined by the polarizability of Pb^{2+} ions.[12] The effect of increase in number of highly polarizable Pb^{2+} ions probably overcomes that of decrease in oxygen coordination number of Pb^{2+} ions.

4.3 IR transmission

The cutoff wavelength in IR region of 67PbO·33GaO$_{1.5}$ glass is longer than that of 67PbO·33SiO$_2$ glass. The cutoff wavelength in IR region of oxide glasses is mainly determined by the absorption due to the fundamental cation-oxygen ion stretching vibrations. According to the theory of diatomic molecules,[1]

$$\lambda \propto \left(\frac{\mu}{E_s}\right)^{1/2} \tag{6}$$

where λ, μ and E$_s$ represent the cutoff wavelength in IR region, the reduced mass represented by m$_c$m$_o$/(m$_c$ + m$_o$) and the cation-oxygen single bond strength, respectively; m$_c$ and m$_o$ represent masses of cation and oxygen, respectively. The calculated $(\mu/E_s)^{1/2}$ of Pb-O, Ga-O and Si-O are 0.64, 0.44 and 0.31, respectively, where the values reported by Sun are used as the cation-oxygen single bond strength.[28] The 1.5 times larger value of $(\mu/E_s)^{1/2}$ for Ga-O than Si-O results in the 1.6 times longer cutoff wavelength of 67PbO·33GaO$_{1.5}$ glass than that of 67PbO·33SiO$_2$ glass. The substitution of SiO$_2$ by heavier oxides, Ga$_2$O$_3$ in the present case, is confirmed to be useful for high IR-transmitting glasses.

4.4 Nonlinear optical properties

The $\chi^{(3)}$ value of 67PbO·33GaO$_{1.5}$ glass is about 1.7 times higher than those of 67PbO·33SiO$_2$ and 60PbO·40BO$_{1.5}$ glasses. This is attributed to the substitution of Ga$_2$O$_3$ for SiO$_2$ or B$_2$O$_3$. The THG intensity of 67PbO·33GaO$_{1.5}$ glass is not so different from those of 67PbO·33SiO$_2$ and 60PbO·40BO$_{1.5}$ glasses. However, the coherent length of 67PbO·33GaO$_{1.5}$ glass is considerably shorter than other two glasses, which results in the highest $\chi^{(3)}$ value of 67PbO·33GaO$_{1.5}$ glass.

The $\chi^{(3)}$ values of the above three PbO-based glasses are about 20 – 30 times higher than that of SiO$_2$ glass. This is probably due to the high contents of Pb^{2+} ions of large polarizability. Considerably lower values of calculated $\chi^{(3)}$ than observed $\chi^{(3)}$ may indi-

cate that the empirical equation for calculating $\chi^{(3)}$ (Eqs.(4), (5)) cannot be applied to the glasses containing a very high concentration of extremely polarizable ion such as Pb^{2+}. It has been reported that Li_2O-TiO_2-TeO_2 ternary oxide glasses show high $\chi^{(3)}$ values of $3.4-8.0 \times 10^{-13}$ esu.[29] The prsent values of 7.7×10^{-13} esu for $67PbO \cdot 33GaO_{1.5}$ glass is comparable to those glasses.

4.5 Crystallization

It is seen from DSC and X-ray diffraction measurements that the process of crystallization of the glasses changes at the composition of 50 mol% PbO. The profile of the DSC curves of PbO-$GaO_{1.5}$ glasses drastically changes between the compositions of 50 and 60 mol% PbO. Although T_g linearly decreases with the PbO content, T_x drastically decreases for the compositions of more than 50 mol% PbO. In addition, $(T_x$-$T_g)$ shows a maximum value at 50 mol% PbO.

The DSC curves of $40PbO \cdot 60GaO_{1.5}$ and $50PbO \cdot 50GaO_{1.5}$ glasses show one sharp peak. It is assumed from X-ray diffraction patterns that this peak corresponds to the formation of α-PbO. The small ripple at about 570°C in the DSC curve of $50PbO \cdot 50GaO_{1.5}$ glass probably reflects the formation of $PbGa_2O_4$ or the transformation of α-PbO to βPbO. It is expected from the DSC curve that $40PbO \cdot 60GaO_{1.5}$ glass shows similar crystallization behavior.

On the other hand, β-PbO is first precipitated in $60PbO \cdot 40GaO_{1.5}$ glass. It should be noted that the observed d-spacings of β-PbO are smaller than the values for pure β-PbO by about 0.02 in the samples heated at 430, 450 and 500°C. This may indicate that a β-PbO-like solid solution containing Ga is formed in the region from 430 to 500°C. The broad exothermic peak at about 480°C in the DSC curve probably reflects the formation of this solid solution. It is assumed from the X-ray pattern for 550°C that the relatively sharp peak at about 530°C in the DSC curve may mainly reflect the transformation of the β-PbO-like solid solution to α-PbO. At the same time, pure β-PbO crystal is assumed to form at higher temperatures than 550°C. The small ripple observed at higher temperatures than 550°C in the DSC curve may be related to the formation of $PbGa_2O_4$ crystal.

Only α-PbO, β-PbO and $PbGa_2O_4$ crystals are precipitated in the process of crystallization of PbO-$GaO_{1.5}$ glasses, which is consistent with the phase diagram on the PbO-Ga_2O_3 system.[30] The detailed crystallization behavior of PbO-$GaO_{1.5}$ glasses is now under investigation.

4.6 Raman spectra

The 510 cm^{-1}-band in Raman spectra is assigned to the bending vibration of the Ga-O-Ga bond connecting GaO_4 tetrahedra.[6] The peak wavenumber of 510 cm^{-1}-band slightly decreases with increasing PbO content. It has been reported that the variation of the peak wavenumber of 510 cm^{-1}-band largely depends on the ionic field strength of network-modifying cations rather than Ga-O bond strength.[13] However, the effect of Ga-O bond strength is appreciable in the Raman spectra of PbO-$GaO_{1.5}$ glasses obtained in the present study. The decrease in the peak wavenumber of 510 cm^{-1}-band may indicate that the Ga-O bond strength becomes weak with increasing PbO content.

The strongest 400 cm^{-1}-band among all the bands is assigned to Ga-O-Pb vibration.[13] The 400 cm^{-1}-band shifts to lower wavenumbers with increasing PbO content, indicating that the average bond strength of Ga-O may become weak with increasing PbO content. It

should be noted that the intensity ratio of the 400 cm^{-1}-band to 510 cm^{-1}-band, I(400)/I(510), is nearly constant for all the compositions, indicating that the number of Ga-O-Ga bond in the glasses may be constant for different compositions. In other words, all the sites next nearest to Ga^{3+} ions should not be occupied by Pb^{2+} and Ga^{3+} ions.

The 620 cm^{-1}- and 720 cm^{-1}-bands are assigned to the stretching vibrations involving non-bridging oxygens of GaO$_4$ tetrahedra.[6] The presence of these bands indicates that non-bridging oxygens are formed on introduction of PbO. It has been reported that the fraction of GaO$_4$ tetrahedra having non-bridging oxygens increases with increasing content of network-modifying oxides in alkali and alkaline earth gallate glasses.[6] On the other hand, the authors reported that the fraction of non-bridging oxygens in GaO$_4$ tetrahedra decreases with increasing PbO and BiO$_{1.5}$ contents in PbO-BiO$_{1.5}$-GaO$_{1.5}$ glasses.[13] In the present glasses, the ratio of intensities of the 620 cm^{-1}- and 700 cm^{-1}-band to the 510 cm^{-1}-band, I(620,700)/I(510), decreases with increasing PbO content. This indicates that the fraction of non-bridging oxygens in GaO$_4$ tetrahedra decreases with increasing PbO content, and at higher contents of Pb^{2+} ions they participate in glass network as network former. Briefly, the substantial fraction of oxygens given to GaO$_4$ tetrahedra from PbO may decrease, resulting in a decrease of the average number of non-bridging oxygens in GaO$_4$ tetrahedra. This, in turn, will cause an increase in fraction of Pb^{2+} ions coordinated by three or four oxygens.

5. CONCLUSIONS

The densities, refractive indices, glass-transition temperature, T$_g$, IR transmission, third-order nonlinear susceptibility, $\chi^{(3)}$, and crystallization behavior have been investigated for PbO-GaO$_{1.5}$ glasses, and the structure of the glasses has been discussed on the basis of Raman spectra. The density and refractive index increased and the T$_g$ decreased with increasing PbO content of the glasses. The cutoff wavelength in IR region of 67PbO·33GaO$_{1.5}$ glass was longer than that of 67PbO·33SiO$_2$ glass. The $\chi^{(3)}$ value of 67PbO·33GaO$_{1.5}$ glass was about 1.7 times higher than that of 67PbO·33SiO$_2$ glass. Heating of the glasses caused the precipitation of α-PbO crystal and β-PbO-like solid solution for 50PbO·50GaO$_{1.5}$ and 60PbO·40GaO$_{1.5}$ glasses, respectively. Raman spectra of the glasses indicated that Ga^{3+} ions are tetrahedrally coordinated and the Ga-O bond strength decreases with increasing PbO content. It was also indicated that the sites next nearest to Ga^{3+} ions are occupied by not only Pb^{2+} ions but also Ga^{3+} ions in even very high-PbO composition and the fraction of non-bridging oxygens in GaO$_4$ tetrahedra decreases with increasing PbO content.

REFERENCES

(1) T. Kokubo, M. Nishimura and M. Tashiro, *J. Non-Cryst. Solids,* **22,** 125 (1976).

(2) T. Kokubo, Y. Inaka and S. Sakka, *J. Non-Cryst. Solids,* **80,** 518 (1986).

(3) K. Fukumi, T. Kokubo, K. Kamiya and S. Sakka, *J. Non-Cryst. Solids,* **84,** 100 (1986).

(4) F. Miyaji, K. Fukumi and S. Sakka, *J. Ceram. Soc. Jpn. Inter. Ed.,* **97,** 263 (1989).

(5) E.M. Vogel, *J. Am. Ceram. Soc.,* **72,** 719 (1989).

(6) K. Fukumi and S. Sakka, *Phys. Chem. Glasses,* **29,** 1 (1988).

(7) T. Yoko, K. Kamiya, T. Tanaka and S. Sakka, *J. Ceram. Soc. Jpn.,* **97,** 289 (1989).

(8) W.H. Dumbaugh, *Phys. Chem. Glasses,* **27,** 119 (1986).

(9) T. Komatsu, R. Sato, K. Imai, K. Matusita and T. Yamashita, *J. Non-Cryst. Solids, Jpn. J. Appl. Phys.,* **27,** L550 (1988).

(10) F. Miyaji, T. Yoko and S. Sakka, *J. Non-Cryst. Solids,* **126,** 170 (1990).

(11) T. Minami, *J. Non-Cryst. Solids,* **95&96,** 107 (1987).

(12) F. Miyaji, K. Tadanaga, T. Yoko and S. Sakka, Proceedings of the International Conference on Science and Technology of New Glasses, 376 (1991).

(13) F. Miyaji and S. Sakka, *J. Non-Cryst. Solids,* **134,** 77 (1991).

(14) F. Miyaji, K. Tadanaga, T. Yoko and S. Sakka, submitted to *J. Non-Cryst. Solids.*

(15) J.E. Shelby, *J. Am. Ceram. Soc.,* **71,** C254 (1988).

(16) P.D. Maker, R.W. Terhune, M. Nisenoff and C.M. Savage, *Phys. Rev. Lett.,* **8,** 21 (1962).

(17) D.A. Long, "Raman Spectroscopy", McGraw-Hill, London, 1977, P. 82–84.

(18) K. Fukumi and S. Sakka, *J. Non-Cryst. Solids,* **95&96,** 193 (1987).

(19) E. Kordes, *Z. Anorg. Allg. Chem.,* **241,** 1 (1939).

(20) "Handbook of glass data Part A", O.V. Mazurin, M.V. Streltsina and T.P. Shvaiko-Shvaikovs-kaya Ed., Elsevier, Amsterdam, 1983, P. 467–483.

(21) K. Kubodera and H. Kobayashi, *Mol. Cryst. Liq. Cryst.,* **182A,** 103 (1990).

(22) G.R. Meredith, B. Buchalter and C. Hanzilk, *J. Chem. Phys.,* **78,** 1533 (1983).

(23) R. Adair, L.L. Chase and A. Payne, *J. Opt. Soc. Am. B,* **4,** 875 (1987).

(24) S. Geller, *J. Chem. Phys.,* **33,** 676 (1960).

(25) M.I. Kay, *Acta Cryst.,* **14,** 80 (1961).

(26) J.C. Lapp, W.H. Dumbaugh and M.L. Powley, *Rivista della Staz. Sper. Vetro,* **1,** 91 (1989).

(27) L.E. Topol, D.H. Hengstenberg, M. Blander, R.A. Happe, N.L. Richardson and L.S. Nelson, *J. Non-Cryst. Solids,* **12,** 377 (1973).

(28) K.H. Sun, *J. Am. Ceram. Soc.,* **30,** 277 (1947).

(29) H. Nasu, Y. Ibara and K. Kubodera, *J. Non-Cryst. Solids,* **124,** 275 (1990).

(30) M. Nevriva, E. Pollert and K. Fischer, *Mat. Res. Bull.,* **13,** 473 (1978).